

# Transverse deflecting cavities

*G. Burt*

Lancaster University, Lancaster, UK

## Abstract

Transverse deflecting cavities are used for a number of applications in modern accelerators. In this paper we discuss the fields of these cavities, some of their applications, and some important aspects of their design.

## 1 Introduction

Transverse deflecting cavities are required in accelerators for a variety of applications that require a time-varying transverse deflection of charged particles. To provide a transverse force to charged particles we must provide transverse electric fields,  $E$ , transverse magnetic fields,  $B$ , or both as given by the Lorentz force equation,  $F = q(E + v \times B)$  where  $q$  is the particles' charge and  $v$  is the particle velocity. As the particles travel in the  $z$  direction, for a horizontal force we require a horizontal electric field and/or a vertical magnetic field.

For a pillbox cavity the transverse fields of mode  $TM_{mnp}$  vary transversely as  $J_m(k_t r) \sin(m\phi)$  for  $B_r$  and  $E_\phi$  and  $J'_m(k_t r) \cos(m\phi)$  for  $B_\phi$  and  $E_r$  where  $k_t$  is the transverse wavenumber. Also the transverse fields of mode  $TE_{mnp}$  vary transversely as  $J'_m(k_t r) \cos(m\phi)$  for  $B_r$  and  $E_\phi$  and  $J_m(k_t r) \sin(m\phi)$  for  $B_\phi$  and  $E_r$  where  $k_t$  is the transverse wavenumber. Hence only modes of order  $m = 1$ , the dipole modes, have non-zero transverse fields at  $r = 0$ , the cavity centre. Monopole modes such as the accelerating  $TM_{010}$  mode of a pillbox cavity only have longitudinal fields on axis so they cannot be used to deflect the beam if the beam travels down the centre.

Most dipole modes have both transverse electric and transverse magnetic fields at  $r = 0$ , however, these two fields can either add constructively or cancel each other out. In order to find the transverse kick for ultra-relativistic particles we instead use the Panofsky–Wenzel theorem [1] which relates the transverse voltage  $V_x$  to the transverse variation of the longitudinal electric field.

$$V_x = \int \frac{F_x}{q} \cdot dz = \int (E_x + c \times B_y) \cdot dz = -\frac{ic}{\omega} \int (\nabla_t E_z) \cdot dz . \quad (1)$$

This equation is valid for all cavities and is not constrained to pillbox cavities. Note that this is not a real voltage as some of the force comes from the magnetic field, it is really transverse work per unit charge. As the transverse voltage is proportional to the gradient of  $E_z$  it is clear that TE modes, which do not have longitudinal electric fields, cannot be used to provide a transverse deflection of ultra-relativistic particles. To deflect ultra-relativistic particles using a pillbox cavity we must use TM dipole modes. TE modes can be used to deflect low-velocity particles or to make RF undulators but will not be discussed here.

The lowest frequency dipole modes pillbox cavities are usually the  $TE_{111}$  mode and the  $TM_{110}$  mode. The  $TE_{111}$  mode has both transverse electric and magnetic fields on axis, perpendicular to each other, however, as already mentioned they both exactly cancel each other out. The  $TM_{110}$  mode has zero electric field on axis but has a large transverse magnetic field which is used to provide the transverse force. In a pillbox cavity the dipole fields of a  $TM_{110}$  mode are given by

$$\begin{aligned}
E_z &= E_0 J_1(k_t r) \cos(\varphi), \\
H_r &= \frac{-i\omega\epsilon}{k_t^2 r} E_0 J_1(k_t r) \sin(\varphi), \\
H_\varphi &= \frac{-i\omega\epsilon}{k_t} E_0 J_1'(k_t r) \cos(\varphi).
\end{aligned} \tag{2}$$

The addition of the beam-pipes and irises causes the  $TM_{110}$  mode in the cavity to couple to a  $TE_{11}$ -like mode in the iris causing a transverse electric field to appear on axis, making the mode a hybrid mode as can be seen in Fig. 1. This interaction has a marked effect on the dispersion curves of the  $TM_{110}$ -like and  $TE_{11}$ -like modes of the cavity, which we discuss later. An electron travelling through the cavity at close to the speed of light will experience the electric fields in the iris and the magnetic fields in the cavity, however, as the cell periodicity is usually half the wavelength and the electric and magnetic fields are 180 degrees out-of-phase in standing wave cavities, the forces due to the two fields act in the same direction for deflecting mode cavities. The fields near the cavities' axis of longitudinal symmetry are given by [2]

$$\begin{aligned}
E_x &= E_0 \frac{k}{4} (a^2 + x^2 - y^2) \sin z \cos \omega t, \\
E_y &= E_0 \frac{k}{2} xy \sin kz \cos \omega t, \\
E_z &= E_0 x \cos kz \cos \omega t;
\end{aligned} \tag{3a}$$

$$\begin{aligned}
cB_x &= E_0 \frac{k}{2} xy \cos kz \sin \omega t, \\
cB_y &= -E_0 \frac{1}{k} \left( \frac{(ka)^2}{4} - 1 + \frac{k^2(x^2 - y^2)}{4} \right) \cos kz \sin \omega t, \\
cB_z &= -E_0 y \sin kz \sin \omega t.
\end{aligned} \tag{3b}$$

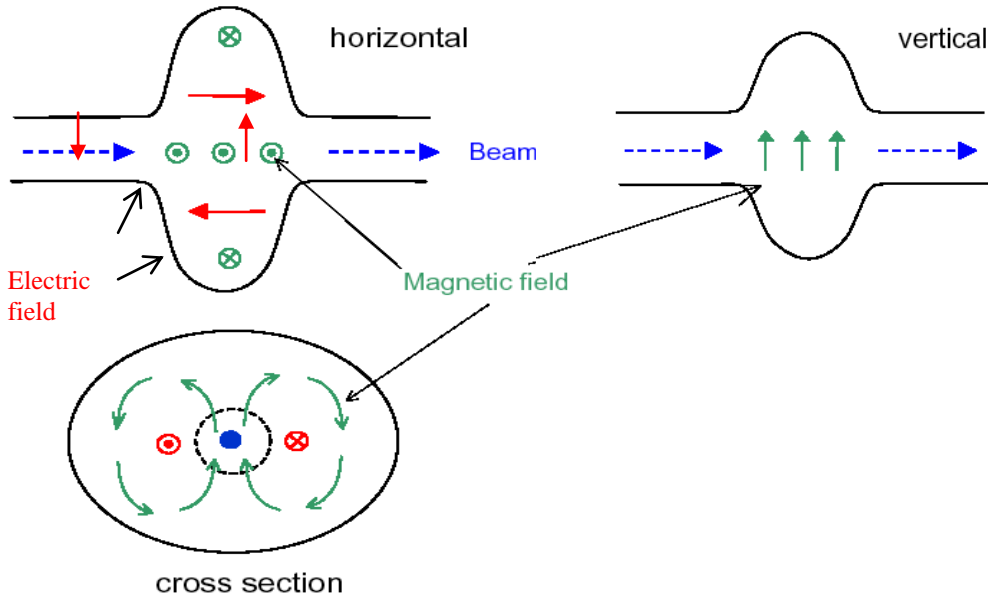


**Fig. 1:** Electric and magnetic fields in a dipole cavity

For the  $TM_{110}$ -like dipole modes we can insert Eq. (3a) into Eq. (1) to obtain the relationship between  $V_t$  and  $V_z$

$$V_x = -\frac{ic}{\omega} \int_0^L dz \nabla_r E_z(z, z/c) = -\frac{ic}{\omega} \frac{[V_z(x) - V_z(0)]}{x} = -\frac{ic}{\omega} \frac{V_z(x)}{x} \quad (4)$$

For an azimuthally symmetric cavity  $V_z$  is zero at the cavity centre. The definition of a transverse voltage leads to the definition of a transverse  $(R/Q)_t$  which is useful for relating the transverse voltage  $V_\perp$  to the stored energy  $U$  and longitudinal voltage  $V_z$  at an off-axis distance of  $a$  in the cavity

$$\left(\frac{R}{Q}\right)_t = \frac{|V_x|^2}{2\omega U} = \frac{|V_z(a)|^2}{2\omega U} \left(\frac{c}{\omega a}\right)^2. \quad (5)$$

## 2 Transverse kicks and rotations

The transverse offset of a bunch that has been kicked by a transverse deflecting cavity is dependent on the beam optics between the cavity and the point where we measure the offset. The relationship between a particle's transverse position and velocity between two positions is given by the transfer matrix,  $R$ .

$$\begin{pmatrix} x \\ x' \\ y \\ y' \end{pmatrix}_{\text{final}} = \begin{pmatrix} R_{11} & R_{12} & R_{13} & R_{14} \\ R_{21} & R_{22} & R_{23} & R_{24} \\ R_{31} & R_{32} & R_{33} & R_{34} \\ R_{41} & R_{42} & R_{43} & R_{44} \end{pmatrix} \begin{pmatrix} x \\ x' \\ y \\ y' \end{pmatrix}_{\text{initial}}. \quad (6)$$

The particle with a transverse velocity of zero before the deflecting cavity which leaves the cavity at an angle,  $x'$  will have an offset at a later point,  $\Delta x$ , given by

$$\Delta x = R_{12}x'. \quad (7)$$

If we apply a transverse voltage in the horizontal plane  $V_x$  to an ultra-relativistic electron beam of energy  $E$ , the angle at which it leaves the cavity will be given by

$$x' = \frac{V_x}{E}. \quad (8)$$

Hence the offset of this particle at a later point will be given by

$$\Delta x = R_{12} \frac{eV_x}{E}. \quad (9)$$

Transverse deflecting cavities can also be used to rotate bunches as well as deflect them as they can deliver a sinusoidal time-varying transverse voltage. If we consider a number of charged particles that leave a deflecting cavity at a time  $t$ , the offset of these particles at a position further down the accelerator is given by

$$\Delta x = R_{12} \frac{eV_x \sin(\omega t)}{E}, \quad (10)$$

where  $\omega$  is the resonant frequency of the cavity. Hence a particle leaving the cavity at time  $t = 0$  will not experience a transverse kick while particles leaving the cavity at times  $t = -\pi/2\omega$  and  $t = \pi/2\omega$  will experience equal and opposite kicks, hence the bunch will appear to have rotated about the particle which left the cavity at  $t = 0$ . If the bunch duration  $\sigma_t$  is small compared to the period of the RF then the rotation  $\theta$  is given by

$$\theta \approx \frac{\Delta x}{c\sigma_t} \approx R_{12} \frac{eV_x \sin(\omega\sigma_t)}{c\sigma_t E} \approx R_{12} \frac{eV_x \omega}{cE}. \quad (11)$$

Deflecting mode cavities phased to give bunch rotations rather than deflections are known as crab cavities.

### 3 Applications of transverse deflecting cavities

#### 3.1 RF separators

The first transverse deflecting cavities were used as RF separators, which were able to separate particles of different masses [3]. Each particle traversing the cavity receives an additional transverse momentum kick, but particles of different masses, such as kaons and protons, will be deflected at different angles. This leads to a transverse separation between the two particle species which can be used to separate them for detection. One such system proposed at FNAL uses two deflecting cavities separated by a lens system [4]. The first cavity provides a transverse kick to all particles which then travel through the lens system; as the pions, kaons, and protons will all arrive at the second cavity at different times they will all receive differing kicks. The pions and protons are deflected into a beam stopper and the kaons are deflected to a detector. For this scheme the phase separation between the pions and kaons,  $\Delta\phi$ , is given by

$$\Delta\phi = \omega \frac{L}{c} \left( \frac{1}{\beta_K} - \frac{1}{\beta_\pi} \right), \quad (12)$$

where  $\omega$  is the angular frequency of the RF cavity,  $L$  is the distance between the two RF systems,  $c$  is the speed of light, and  $\beta_x$  is the normalized velocities of the kaons and pions.

Another application of transverse separators is to separate trains of electrons to send them to different detectors, insertion devices, or for use in ERLs [5]. In such a system the RF frequency of the deflecting cavity is a sub-harmonic of the bunch separation, hence several bunches traverse the cavity in one RF period. Each of these bunches will arrive at a different phase and hence will receive a different transverse kick, allowing bunches to be separated.

#### 3.2 RF-cavity-based bunch length diagnostics

If we alter the phase of a transverse deflecting cavity, instead of deflecting the whole bunch, we can introduce a correlation between a particle's transverse momenta and its longitudinal position in the bunch. This property can be exploited for use in a bunch length diagnostic measurement where the bunch is deflected onto a screen and the bunch length can hence be calculated by the voltage gradient across the bunch and the transverse size of the bunch on the screen [6]. One must be careful that the transverse deflection causes the bunch to be sufficiently spread out transversely at the screen such that the transverse bunch size doesn't dominate the measurement. The temporal resolution,  $\Delta t$  of such a measurement is given by

$$\Delta t = \sigma_x \frac{2mc^2\gamma}{L\omega eV_x}, \quad (13)$$

where  $\sigma_x$  is the bunch width,  $\gamma$  is the relativistic mass correction,  $L$  is the distance between the cavity and the screen,  $e$  is the charge of the electron, and  $V_t$  is the transverse voltage [7].

#### 3.3 Crab cavities for colliders

In circular colliders such as KEK-B and the LHC the colliding beams circulate in two separate beam-lines; at the interaction region (IR) the two beams are brought together with a finite crossing angle and then separated again. Also the next generation of electron-positron colliders (ILC and CLIC) are proposed to utilize a finite crossing angle at the interaction

region (IR) to simplify extraction of the spent beam. However, these finite crossing angles reduce the luminosity of the collision as the two beam cross-sections do not completely overlap. Simple geometric arguments can be used to show that the luminosity reduction factor  $S$  can be given as

$$S = \frac{1}{\sqrt{1 + \left(\frac{\sigma_z \theta_c}{2\sigma_x}\right)^2}}, \quad (14)$$

where  $\theta_c$  is the full crossing angle,  $\sigma_x$  is the bunch width, and  $\sigma_z$  is the bunch width [8]. In order to correct for the finite crossing angle it is necessary to rotate the bunch prior to the IR. One method of rotating the bunches, suggested by R. Palmer [9], is to use crab cavities. Crab cavities are a subset of transverse deflecting cavities, where the bunch centre traverses the cavity at the zero kick phase. Owing to the finite size of the bunch only the centre does not receive a kick, the head and tail of the bunch receive equal and opposite kicks.

For linear colliders the required voltage can be calculated by considering the required offset of an electron at the head of a bunch at the IR,  $\Delta x$ , in order for the beam to have the correct rotation. From this offset we can use the  $R_{12}$  transfer matrix component between the crab cavity location and the IR to estimate the required transverse voltage,  $V_t$ .

$$\theta_{crab} = \frac{\Delta x (\sigma_z)}{\sigma_z} \approx \frac{\omega}{c} R_{12} \frac{eV_x}{E}. \quad (15)$$

Here  $E$  is the beam energy,  $\omega$  is the frequency of the cavity, and  $c$  is the speed of light [8]. As can be seen, increasing the  $R_{12}$  matrix component, which relates  $x'$  at the cavity to  $\Delta x$  at the IR, reduces the required voltage, hence crab cavities tend to be placed at locations with a high  $R_{12}$ . This can lead to problems since instabilities at the cavity, such as RF phase errors and wakefields, can be magnified at the IR.

For circular colliders there are two possible scenarios for crab cavities, a local scheme and a global scheme. In a local scheme the beam is rotated by a crab cavity close to the IR and straightened by a second crab cavity placed on the other side of the IR, each at a phase advance of  $\pi/2$  from the IR. For this case the voltage required from the first cavity  $V_1$  is

$$V_1 = \frac{c^2 p_s \tan\left(\frac{\theta_c}{2}\right)}{q\omega\sqrt{\beta^* \beta_{crab}} \sin(\Delta\phi_0)}, \quad (16)$$

where  $p_s$  is the particle momentum,  $q$  is the particle charge,  $\beta^*$  is the beta function at the IR,  $\beta_{crab}$  is the beta function at the crab cavity, and  $\Delta\phi_0$  is the phase advance between the cavity and the IR [10]. The voltage required from the second cavity  $V_2$  is

$$V_2 = -R_{22} V_1. \quad (17)$$

Alternatively a global scheme can be used where a single crab cavity is used per beam-line to rotate the bunch. As the bunch trajectory is a closed orbit, the bunch will rotate as it travels round the ring achieving the correct rotation at the IR. For this scheme the required voltage is

$$V = \frac{c^2 p_s \tan\left(\frac{\theta_c}{2}\right)}{q\omega\sqrt{\beta^* \beta_{crab}}} \left| \frac{2\sin(\pi Q)}{\cos(\Delta\phi_0 - \pi Q)} \right| \quad (18)$$

where  $Q$  is the betatron tune of the storage ring [10].

For both circular and linear crab cavities the cavity roll alignment is critical. If the cavity is misaligned the crab cavity will create a crossing angle in the vertical plane. The luminosity reduction factor for a roll misalignment of  $\varphi_{\text{roll}}$  is given by

$$S = \frac{1}{\sqrt{1 + \frac{\sigma_z \theta_c \sin \varphi_{\text{roll}}}{2\sigma_y}}}. \quad (19)$$

For beams that are focused down to nanometre-scale beam sizes in the vertical plane at the IP, the roll alignment can be very tight.

### 3.4 Light sources

Recently there has been much interest in producing short X-ray pulses from light sources. The majority of the designs use linear FELs, however, producing X-rays from storage rings may be cheaper and simpler. There are well-known difficulties in producing short X-ray pulses in storage rings due to the longer bunch lengths, however, a scheme proposed by Zholents using crab cavities may make this possible [11]. In this scheme an initial crab cavity is used to produce a chirp on the bunch, where the vertical momenta of the particles in the bunch are correlated to their longitudinal position. If an undulator is placed downstream of this crab cavity then the photons produced will have a correlation between their vertical position and time, and can hence be shortened using vertical slits or compressed using asymmetrically cut crystals. A second crab cavity is required at a vertical phase advance of  $n\pi$  from the first cavity in order to remove the transverse momentum in order to stop emittance growth as the bunch traverses around the ring.

### 3.5 Emittance exchange

The transverse variation in accelerating voltage can also be used to reduce longitudinal emittance at the expense of transverse emittance or vice versa. If a beam of charged particles is passed through the first two magnets of a chicane before the dipole cavity, the particles will be offset in the cavity with displacement proportional to their energy. Owing to the transverse variation in accelerating voltage, particles with energy higher than the design energy will be decelerated and particles with lower energy will be accelerated, reducing the energy spread of the beam. However, as the accelerating voltage is in phase with the crabbing voltage, the beam will also obtain a time-dependent kick causing the transverse emittance to grow [12].

## 4 Dispersion and equivalent circuit of dipole modes

To analyse the band structure of most multi-cell cavities an equivalent circuit is traditionally used. For accelerating cavities a single chain of LC resonators which are capacitively coupled can be used to accurately predict the modal frequencies and cell amplitudes. For dipole modes the crabbing mode is made up from a mixture of TE and TM modes, hence a single chain of resonators is not sufficient to model such a cavity. For dipole modes a better fit can be made by utilising a double chain model of LC resonators [13], one for the TE mode and one for the TM mode, coupled inductively (where a negative inductance can represent a capacitive coupling) as shown in Fig. 2. This circuit has two solutions giving a TM-like hybrid pass-band and a TE-like hybrid pass-band.

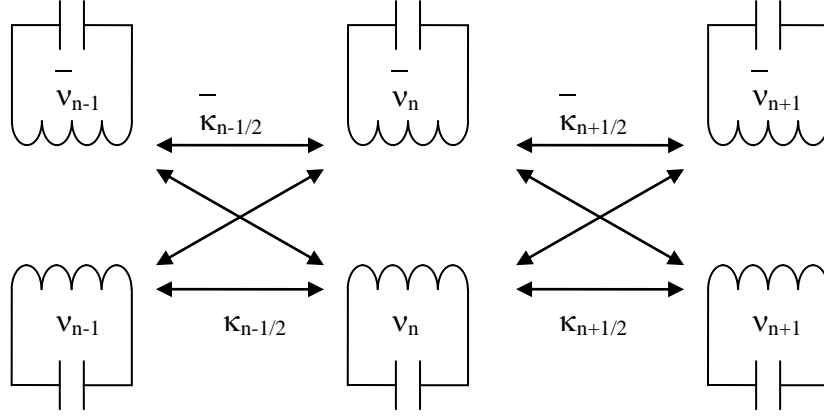


**Fig. 2:** Two-chain equivalent circuit model of a dipole cavity

The circuit equation for the  $m$ th cell of this circuit is

$$\begin{aligned} \left( \frac{1}{\nu^2} - \lambda \right) f_m - \frac{\kappa}{2} f_{m+1} - \frac{\kappa}{2} f_{m-1} &= -\frac{\sqrt{\kappa\bar{\kappa}}}{2} f_{m+1} + \frac{\sqrt{\kappa\bar{\kappa}}}{2} f_{m-1} \\ \left( \frac{1}{\bar{\nu}^2} - \lambda \right) \bar{f}_m - \frac{\bar{\kappa}}{2} \bar{f}_{m+1} - \frac{\bar{\kappa}}{2} \bar{f}_{m-1} &= \frac{\sqrt{\kappa\bar{\kappa}}}{2} \bar{f}_{m+1} - \frac{\sqrt{\kappa\bar{\kappa}}}{2} \bar{f}_{m-1} \end{aligned}, \quad (20)$$

where  $f$  and  $\bar{f}$  are the amplitude variables,  $\lambda = 1/\nu^2$  is the eigenvalue,  $\nu$  and  $\bar{\nu}$  are the frequencies,  $\kappa$  and  $\bar{\kappa}$  are the intra-chain coupling factors, and  $\sqrt{\kappa\bar{\kappa}}$  is the inter-chain coupling factor. The terms on the LHS are the terms for a chain of resonators while the RHS contains the cross coupling terms.

The values for the variables in these equations can be found by measuring or simulating the eigen-frequencies of the  $\pi$  and 0 modes of both pass-bands [4]. These eigen-frequencies can be used to calculate the variables using the solutions to Eq. (20). There are four separate solutions, two of which are shown below in Eqs. (21a) and (21b), and the other two are the same with branches 1 and 2 interchanged.

$$\begin{aligned} x &= \frac{1}{2}(\lambda_\pi^1 + \lambda_0^1) \\ \bar{x} &= \frac{1}{2}(\lambda_0^2 + \lambda_\pi^2) \\ \kappa &= \frac{1}{2}(\lambda_\pi^1 - \lambda_0^1) \\ \bar{\kappa} &= \frac{1}{2}(\lambda_0^2 - \lambda_\pi^2) \end{aligned} \quad (21a)$$

$$\begin{aligned} x &= \frac{1}{2}(\lambda_\pi^1 + \lambda_0^2) \\ \bar{x} &= \frac{1}{2}(\lambda_0^1 + \lambda_\pi^2) \\ \kappa &= \frac{1}{2}(\lambda_\pi^1 - \lambda_0^2) \\ \bar{\kappa} &= \frac{1}{2}(\lambda_0^1 - \lambda_\pi^2) \end{aligned} \quad (21b)$$

where  $x = 1/\nu^2$ . The dispersion curves for this equivalent circuit model can be given as

$$\begin{aligned}\lambda^1 &= b + \sqrt{b^2 - c} \\ \lambda^2 &= b - \sqrt{b^2 - c}\end{aligned}\quad (22)$$

where

$$\begin{aligned}b &= \frac{1}{2}(x + \bar{x} - (\kappa - \bar{\kappa})\cos(\phi)) \\ c &= x\bar{x} - \kappa\bar{\kappa} + (x\bar{\kappa} - \kappa\bar{x})\cos(\phi)\end{aligned}\quad (23)$$

and  $\phi$  is the phase advance of the mode.

For the uncoupled pass-bands, for example in a cavity with a small iris, the TM modes are magnetically coupled and the TE modes are electrically coupled; however, the intra-chain coupling is small because the iris is small. As the iris size increases, the intra-chain coupling increases but the TE pass-band drops in frequency and the cross coupling increases. When the two pass-bands are close in frequency the two pass-bands do not cross over, instead the TE pass-band pushes the TM modes with low phase advance downwards in frequency, known as an avoided crossing. This initially reduces the coupling between cells for the lower eigenmode and hence the group velocity to zero. As the iris size increases further, the eigenmode coupling starts to increase again, but with the opposite sign, as the lower band becomes more TE-like, as can be seen in Fig. 3 for an example cavity. This can be problematic as most accelerators require a fairly large cell-to-cell coupling to increase the separation between modes. Moving to larger beam-pipes can increase the coupling, however, this often results in high surface fields.

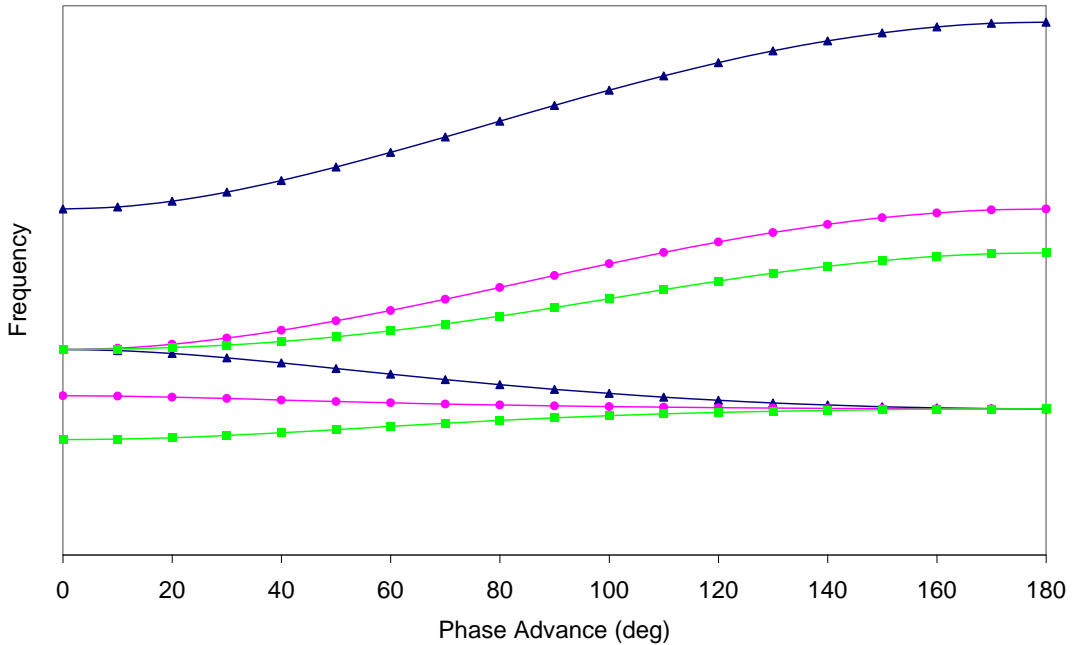


**Fig. 3:** Example dispersion diagrams for a dipole cavity of varying iris radii

## 5 Beam loading in transverse deflecting cavities

In an ideal accelerator there is no beam-loading in dipole cavities as the longitudinal electric field on-axis is zero. However, in real accelerators particle beams rarely travel precisely on-axis and there is usually some offset from the ideal path. The longitudinal electric fields vary linearly with displacement in the plane of deflection for small radial offsets.



$$V_z(x) = ix \frac{\omega V_x}{c}. \quad (24)$$

The power deposited or removed from the cavity from a train of bunches of current  $I_b$  traversing the cavity at a phase  $\omega t$  can then be given as [14]

$$P_{beam} = I_b V_z(x, t) = ix I_b \frac{\omega V_x}{c} e^{i\omega t}, \quad (25)$$

where  $\omega t = 0$  is in phase with the deflecting voltage. It should also be noted that the transverse kick is 90 degrees out-of-phase with the beam loading, hence in a deflecting phase there is no beam-loading and in crabbing phase the beam-loading is maximal. As the longitudinal electric field can be either positive or negative depending on which direction the bunch is offset, the beam-loading can either deposit energy in the cavity or take energy out. The beam loading can vary greatly between bunches if the beam current is sufficiently large and can produce enough power to drive the cavity without an external power (although such a cavity would be unstable). This can cause problems as it means that the power coupler on a crab cavity cannot be matched to the cavity when beam is present as the beam loading cannot be predicted.

## 6 Wakefields in deflecting mode cavities

The transverse kick delivered to the beam from a transverse deflecting cavity has a given polarization, such that the direction of the kick is well defined. However the  $TM_{110}$  in a pillbox is degenerate and has two modes with different polarizations, one in the horizontal plane and one in the vertical plane. A transverse deflecting cavity will utilize one of these modes for its operation. The mode in the opposite polarization to the operating mode is often referred to as the same-order mode (SOM) [15]. As these modes are degenerate they have the same frequency and shunt impedance which can be problematic as the SOM will hence be resonant with the beam and will couple strongly to it. If the modes are at the same frequency, then the SOM will be cut off in the beam-pipe like the operating mode making it difficult to damp; in addition if we use cut-off waveguide or resonant filters to avoid dampers coupling to the operating mode we will also avoid coupling to the SOM as well. In order to separate these two modes we will polarize the cavity in some way, such as using an elliptical cross-section, coupling holes in the iris, or using polarization rods in the cavity. By polarizing the cavity we can shift the SOM to a higher frequency which will move it out of resonance with the beam and make it easier to damp. However, making the cavity strongly asymmetric will reduce the performance of the operating mode, so dampers are often placed in the plane of the SOM so that they do not couple to the operating mode, as it has no fields in that plane. If the dampers do not couple to the operating mode the dampers can avoid using resonant filters or cut-off waveguide and the SOM doesn't need as large a frequency separation for strong damping. This method has an inherent risk associated with it in that if there are mechanical errors in the cavity manufacture the mode polarizations can rotate slightly causing the operating mode to be damped.

In a pillbox cavity with length equal to less than half a wavelength, as is used in most deflecting mode cavities, the  $TM_{110}$  mode is not the first resonant mode in the cavity. The first resonant mode is the  $TM_{010}$  monopole mode which is commonly used in accelerating cavities. As this mode will be at a lower frequency than the operating mode we refer to this cavity as the lower order mode (LOM) and this mode will likely be trapped in the cavity as its frequency will be much lower than the beam-pipe cut-off frequency. This requires the use of special dampers to remove this mode from the cavity. In the KEK-B crab cavity a hollow coaxial beam-pipe couple was utilized where the TEM mode of the coax coupled to the LOM but due to symmetry did not couple to dipole modes [16]. For the ILC crab cavity a hook type coaxial coupler was used. This is similar to the standard F-probe type coaxial coupler used in superconducting cavities except that the end is bent into a hook such that the long tip is bent towards the cavity.

## 7 TEM-type deflecting mode cavities

When we require compact RF cavities it is standard to use TEM-mode coaxial cavities such as quarter-wave or half-wave resonators. Coaxial cavities are not ideal for deflecting mode cavities as they do not have the correct fields for deflection, however, other types of cavities can support TEM modes that have field patterns better suited to deflection. One such cavity is a parallel bar cavity. This cavity is based on a half-wavelength of parallel bar transmission line which can support a TEM mode between the two bars. Each bar has equal and opposite currents and charges so that transverse electric and magnetic fields are created between the bars. However, as all the fields are transverse there is no deflection due to the Panofsky–Wenzel theorem. In order to obtain a deflection we have two options:

1. We can inject the beam into the cavity transversely similar to the approach used in accelerating half-wave resonators [17]. This means that some of the transverse electric field is in the direction of beam propagation as can be seen in Fig. 4. Each bar should be a half wavelength long at the resonant frequency.

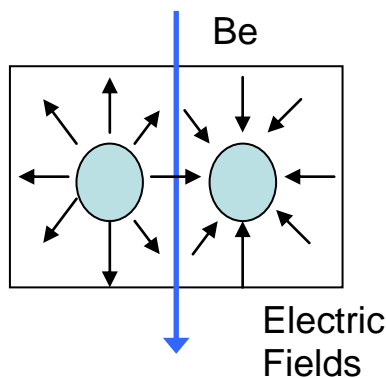


**Fig. 4:** A parallel bar deflecting cavity

2. We can split each bar in the middle creating a longitudinal electric field between the bars, shown in Fig. 5 [18]. The opposing sides of the bar have opposite charges so that the fields constructively add. Each bar should be approximately a quarter wavelength long and the dimensions of the outer do not impact greatly on the performance so this cavity can be very compact. This type of cavity is known as a four-rod deflecting cavity and is currently being used as a beam separator at CEBAF [5]. The advantage of this type of cavity is that the TM-like modes of the cavity are at much higher frequencies compared to the operating mode.

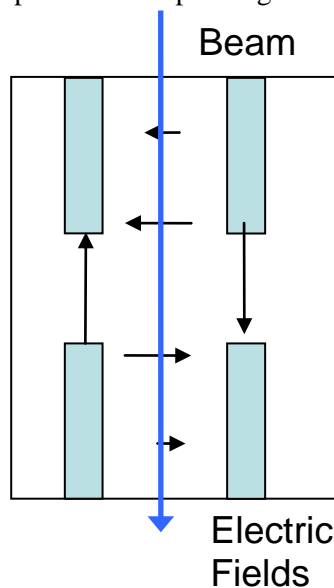


**Fig. 5:** A four-rod deflecting cavity

## References

- [1] W. K. H. Panofsky and W. A. Wenzel, *Rev. Sci. Instrum.* **27** (1956) 967.
- [2] Y. Garault, CERN Report 64-43 (1964).
- [3] A. Micheli and G. Petrucci, Report CERN NP 72-13 (1972).
- [4] M. McAshan and R. Wanzenberg, FERMILAB-TM-2144 (2001).
- [5] C. Hovater, G. Arnold, J. Fugitt *et al.*, JLAB-ACC-96-18 (1996).
- [6] P. Emma *et al.*, SLAC-PUB-8864, August 2000.
- [7] K-J Kim, *in* ICFA Beam Dynamics Mini Workshop Deflecting/Crabbing Cavity Applications in Accelerators, Shanghai, 2008.
- [8] G. Burt, A. C. Dexter, P. Goudket, and A. Kalinin, Effect and tolerances of phase and amplitude errors in the ILC crab cavity, EUROTeV Report 2006-098 (2006).
- [9] R. B. Palmer, SLAC PUB-4707 (1988).
- [10] Y.-P. Sun, F. Zimmermann, R. Toma's, R. Assmann, J. Barranco, T. Weiler, R. Calaga, and A. Morita, *Phys. Rev. Spec. Top. Accel. Beams* **12** (2009) 101002.
- [11] A. Zholents, P. Heimann, M. Zolotarev, and J. Byrd, *Nucl. Instrum. Methods Phys. Res., A* **425** (1999) 385.
- [12] M. Cornacchia and P. Emma, *Phys. Rev. Spec. Top. Accel. Beams* **5** (2002) 084001.
- [13] K. L. F. Bane and R. L. Gluckstern, SLAC-PUB-5783 (March 1992).
- [14] L. Bellantoni and G. Burt, FERMILAB TM-2356 (2006).
- [15] G. Burt *et al.*, *IEEE Trans. Nucl. Sci.* **54** (2007) 1728.
- [16] K. Hosoyama *et al.*, Proceedings of the Asian Particle Accelerator Conference, Tsukuba, Japan, 1998, 6D064.
- [17] J. Delayen and H. Wang, *Phys. Rev. Spec. Top. Accel. Beams* **12** (2009) 062002.
- [18] B. Hall *et al.*, Proceedings of the Particle Accelerator Conference, Vancouver, 2009, TU5PFP040.